PERGAMON

International Journal of Solids and Structures 36 (1999) 1383–1398

INTERNATIONAL JOURNAL OF SOLIDS and STRUCTURES

Two-dimensional elastica analysis of equilibrium shapes of single-anchor inflatable dams

Layne T. Watson[a], Surjani Suherman[b], Raymond H. Plaut[b]

[a]*Departments of Computer Science and Mathematics, Virginia Polytechnic Institute and State University, Blacksburg, VA 24061-0106, U.S.A.*

[b]*Charles E. Via, Jr. Department of Civil Engineering, Virginia Polytechnic Institute and State University, Blacksburg VA 24061-0105, U.S.A.*

Received 14 November 1997; in revised form 12 January 1998

Abstract

Several types of inflatable dams are considered. These are long, air-inflated, cylindrical structures on a rigid foundation. Sometimes one of the long edges of a sheet is folded back to the other edge, and then the two edges are clamped to the foundation along a single anchoring line. A second configuration can be modeled as two sheets attached along two long edges, with one edge anchored and the other free to lift as air pressure is applied between the sheets. Another device treated here is a hinged spillway gate lifted by an inflatable bladder. The cross section of the dam or bladder is analyzed as an inextensible elastica. The governing equations and boundary conditions are formulated for each case, and shooting methods are utilized to obtain numerical solutions for the equilibrium shapes. The effects of the internal air pressure and the external water height are investigated.

1. Introduction

Inflatable dams are sometimes described as sausage-like tubes. They are cylindrical in shape and are usually attached to a concrete foundation and then inflated with air (Tam, 1997). They are made of a nylon-reinforced polymer and their height ranges from 3 to 6 m, while their length may reach 120 m. Approximately 2000 inflatable dams have been constructed, mostly in Japan. There are many uses for inflatable dams, such as creating recreational basins, preventing contamination, increasing groundwater supply, raising the height of existing dams to increase reservoir capacity, and diverting water for irrigation, hydroelectricity, tidal control, or flood control.

Inflatable dams were invented 40 years ago. They often had a double-anchor system, in which

* Author to whom correspondence should be addressed. Tel.: 001 540 231 6072. Fax: 001 540 231 7532. E-mail: rplaut@vt.edu.

0020–7683/99/$ - see front matter
PII: S0020-7683(98)00026-2

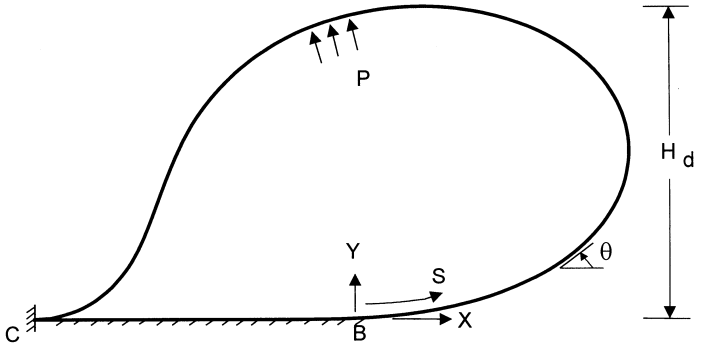

Fig. 1. Geometry of folded dam with no external water.

they were attached to the foundation along two of their generators. Previous studies of the behavior of inflatable dams considered such a support system (see Hsieh and Plaut, 1990; Dakshina Moorthy et al., 1995; Wu and Plaut, 1996; and their reference lists). Recently, these dams have been attached along a single anchor line. The cross section of one type of single-anchor configuration is depicted in Fig. 1. The purpose of the present investigation is to determine the equilibrium shapes of such dams. The forces acting on the dam include the internal air pressure and the external water pressure. The weight of the dam itself is assumed to be negligible compared to these pressures, and friction with the foundation is also neglected.

Two types of inflatable dams are studied here. In the first, analyzed in Section 2, the material is unstrained when it is horizontal, and one end is lifted, folded back, and clamped to the other end and the foundation (point C in Fig. 1). This problem is related to the folding of flexible strips or sheets. Stuart (1966) studied a free-standing fold (or loop) of a flexible material, such as fabric or paper, resting on a horizontal foundation, in order to determine a "bending length". The strip was modeled as an inextensible elastica, and its folded equilibrium shape depended on its flexural rigidity and weight per unit length. Wang (1984) considered lifting a flexible elastic strip and folding it back to form a loop. The last stage of the process is the problem that was treated by Stuart (1996).

Lloyd et al. (1978), Lloyd (1984), and Mahadevan and Keller (1995) considered a flexible sheet that was lowered vertically onto a horizontal surface and formed folds in alternating directions. Again, the last stage of forming of the first fold corresponds to the same free-standing configuration analyzed by Stuart (1966). A related problem was studied by Wang (1981, 1987), in which the weight was neglected and the folded material was held down by a clamp, as in Fig. 1.

In the second type of dam to be treated (Section 3), a thick sheet of material is again unstrained when it is flat. It is slit into two sheets except near one edge. The opposite edge is clamped, and pressure is applied between the two sheets. The edge that was not slit acts as a fin, which is useful in cases of overflow (Mysore et al., 1997; Plaut et al., 1998).

In addition, a type of spillway gate raised by an inflatable bladder is examined (Sehgal, 1996; Plaut et al., 1998). The bladder may be folded back or may have a fin, as described above. For the dams and the gates, the cross section is assumed to behave as an inextensible elastica, as was done in the references just listed for folded strips. The equilibrium shapes are determined numerically

using shooting methods, and the effects of the internal pressure and external water height are determined.

2. Folded dam

2.1. *Without external water*

A portion of the dam with unit width along the generators is considered. The cross section illustrated in Fig. 1 is treated first, with no water present. Both the top and bottom portions of the structure are clamped at C, and the straight section from C to B rests on a rigid horizontal foundation. The horizontal coordinate, X, vertical coordinate Y, and arc length S are measured from B, and $\theta(S)$ is the angle of the tangent with the horizontal. The dam is uniform and inextensible. The perimeter of the cross section is L and the dam has flexural rigidity $D = Eh^3/[12(1-\nu^2)]$, where E is the modulus of elasticity, h is the thickness of the material, and ν is Poisson's ratio. The internal pressure is P and the unknown height of the dam is H_d.

A free body diagram of an element of the cross section from S to $S+\mathrm{d}S$ is depicted in Fig. 2. The horizontal and vertical forces per unit width are F and G, respectively, and the bending moment per unit width is M. From geometry and the assumed moment-curvature relation for an elastica,

$$\frac{\mathrm{d}X}{\mathrm{d}S} = \cos\theta, \quad \frac{\mathrm{d}Y}{\mathrm{d}S} = \sin\theta, \quad \frac{\mathrm{d}\theta}{\mathrm{d}S} = \frac{M}{D}, \tag{1a,b,c}$$

and from equilibrium of the element in Fig. 2,

$$\frac{\mathrm{d}F}{\mathrm{d}S} = -P\sin\theta, \quad \frac{\mathrm{d}G}{\mathrm{d}S} = -P\cos\theta, \quad \frac{\mathrm{d}M}{\mathrm{d}S} = F\sin\theta + G\cos\theta. \tag{2a,b,c}$$

It is assumed that the perimeter L and flexural rigidity D are known. The following non-dimensional quantities are defined with respect to these quantities:

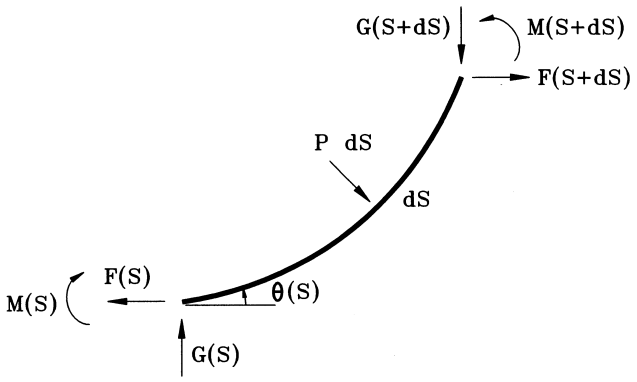

Fig. 2. Element of elastica with horizontal and vertical force components.

$$x = X/L, \quad y = Y/L, \quad s = S/L, \quad h_d = H_d/L,$$
$$p = L^3 P/D, \quad f = L^2 F/D, \quad g = L^2 G/D, \quad m = LM/D. \tag{3}$$

For the free-standing fold studies previously cited, the "bending length" $(D/w)^{1/3}$ is used for nondimensionalization instead of L, where w is the weight per unit area. For a narrow strip, D in this expression is replaced by EI, where I is the moment of inertia, and w is replaced by the weight per unit length.

In first-order form, the nondimensional system of equations to be solved is obtained from (1)–(3) and is given by

$$\frac{dx}{ds} = \cos\theta, \quad \frac{dy}{ds} = \sin\theta, \quad \frac{d\theta}{ds} = m,$$
$$\frac{df}{ds} = -p\sin\theta, \quad \frac{dg}{ds} = -p\cos\theta, \quad \frac{dm}{ds} = f\sin\theta + g\cos\theta. \tag{4a–f}$$

At $s = 0$ (point B in Fig. 1), $x = y = \theta = m = 0$, and at $s = s_C$ (the positive arc length at point C), $x(s_C) = s_C - 1$, $y(s_C) = 0$, $\theta(s_C) = \pi$. Let $z = (f(0), g(0), s_C)$, and $x(s;z)$, $y(s;z)$, etc. denote the solution to (4a–f) with the given initial conditions at $s = 0$. The problem then is to solve the nonlinear system of equations

$$J(z) = (x(s_C;z) - s_C + 1, y(s_C;z), \theta(s_C;z) - \pi) = 0$$

for z. $J(z) = 0$ was solved by a combination of quasi-Newton methods (Moré et al., 1980) and globally convergent homotopy methods (Watson et al., 1998), based on simple shooting and the adjoint equations for (4a–f). Details of the adjoint equations, and of the tandem use of quasi-Newton and homotopy methods, are in Watson (1990) for similar elastica problems.

Equilibrium shapes of the folded dam without external water are presented in Fig. 3 for

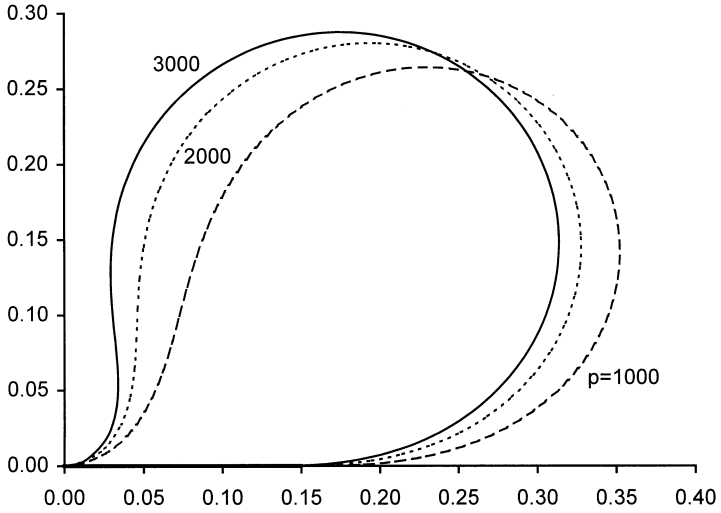

Fig. 3. Equilibrium shapes of folded dam with no external water.

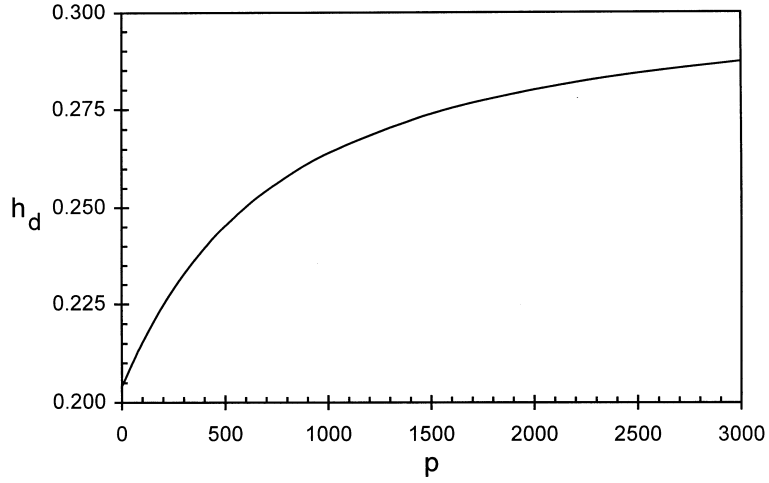

Fig. 4. Influence of internal pressure on height of dam with no external water.

nondimensional internal pressures $p = 1000$, 2000, and 3000. Naturally, the contact length of the elastica with the foundation decreases as p increases. The nondimensional dam height h_d is plotted as a function of p in Fig. 4. When the internal pressure is zero, the similarity solution given by Wang (1981, 1987) is applicable, from which $h_d = 0.204$, $s_C = 0.796$, $f(0) = 19.9$, and $g(0) = 43.7$.

2.2. *With external water*

Now consider the folded dam with external water of height H_w and specific weight Γ on the upstream side, as depicted in Fig. 5. In this case the origin of the coordinate system is placed at point A, located on the dam at the water surface, since the governing equations are different over segments CA and AB. Also, instead of using F and G, the tension per unit width T and shear force

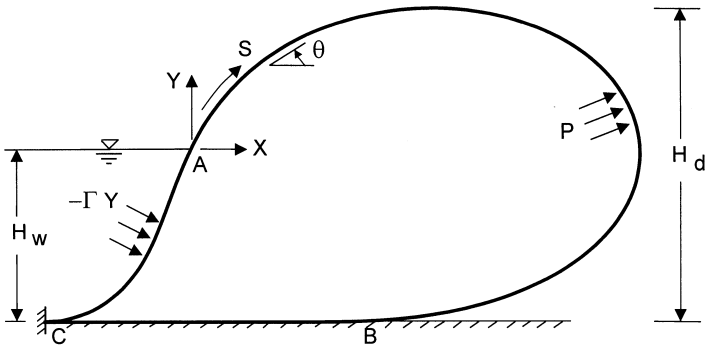

Fig. 5. Geometry of folded dam with external water.

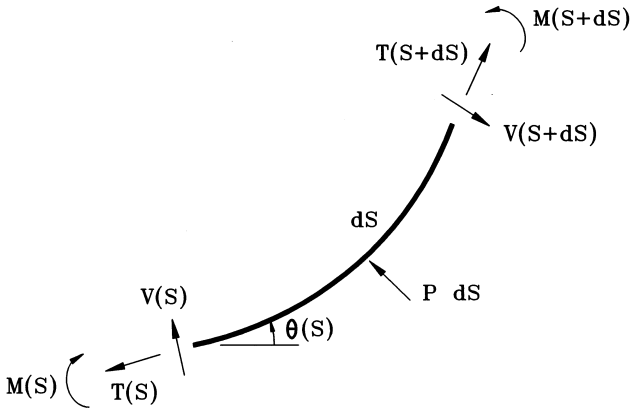

Fig. 6. Element of elastica with tangential and normal force components.

per unit width V are utilized, as defined in the free body diagram of an element in Fig. 6. Equilibrium provides the relations

$$\frac{dM}{dS} = V, \quad \frac{dT}{dS} = -V\frac{d\theta}{dS}, \quad \frac{dV}{dS} = T\frac{d\theta}{dS} + P. \tag{5a,b,c}$$

With the use of (1c) and (5a), one can integrate (5b) and obtain

$$T = T_0 - \frac{1}{2}\frac{M^2}{D}, \tag{6}$$

where T_0 is a constant.

The nondimensional quantities in (3) are used, along with

$$v = L^2V/D, \quad t = L^2T/D, \quad t_0 = L^2T_0/D, \quad h_w = H_w/L, \quad \gamma = L^4\Gamma/D. \tag{7}$$

The governing equations from A (where $s = 0$) to B (where $s = s_B > 0$) in Fig. 5 are given by (4a–c) and

$$\frac{dm}{ds} = v, \quad \frac{dv}{ds} = t_0 m - \frac{1}{2}m^3 + p. \tag{8a,b}$$

From C (where $s = s_C < 0$) to A, the equations are the same except that p is replaced by $p+\gamma y$ (where $y < 0$) in (8b). At $s = 0$, one has $x = y = 0$. The unknowns for this case are

$$z = (\theta(0), m(0), v(0), t_0, s_B, s_C),$$

and the nonlinear system to be solved for z is

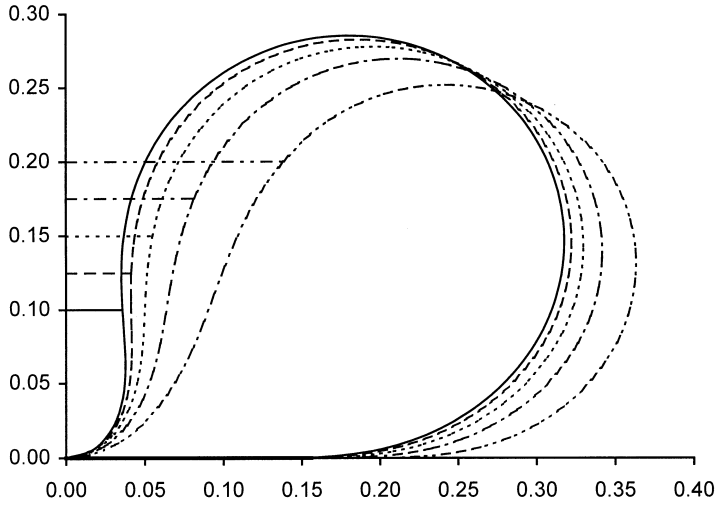

Fig. 7. Influence of external water on equilibrium shape of folded dam for $\gamma = 30{,}000$ and $p = 3000$.

$$J(z) = \begin{bmatrix} y(s_B;z)+h_w \\ \theta(s_B;z)+\pi \\ m(s_B;z) \\ y(s_C;z)+h_w \\ \theta(s_C;z) \\ x(s_B;z)-x(s_C;z)+s_B-s_C-1 \end{bmatrix} = 0,$$

where the last component of J reflects the nondimensional perimeter of 1.

There are numerous equivalent mathematical formulations for the folded dam with external water, most of which are ill posed for shooting. The choice of T and V instead of F and G, and the choice of point A as the shooting origin, were specifically made to obtain a well conditioned system $J(z) = 0$. As above, a combination of quasi-Newton methods (subroutine HYBRJ from MINPACK (Moré et al., 1980)) and homotopy methods (subroutine FIXPNF from HOMPACK90 (Watson et al., 1998)) was used to solve $J(z) = 0$. It is worth mentioning that, despite the advantages of collocation over shooting, a quintic spline collocation formulation (Watson, 1990) of (4a–f) and (4a–c)–(8a,b) was not successful (neither problem is a standard second order boundary value problem). Both quasi-Newton and homotopy methods failed on the spline collocation formulation. Multiple shooting was not tried at all, because generally it is even less robust than collocation.

Equilibrium shapes are plotted in Fig. 7 for nondimensional specific weight $\gamma = 30{,}000$, internal pressure $p = 3000$, and water heights $h_w = 0.1$, 0.125, 0.15, 0.175, and 0.2. Values of t_0, the nondimensional tension per unit width at the lift-off point B, vary from 440 for $h_w = 0.1$ to 394 for $h_w = 0.2$. The case of no external water is given by the solid shape in Fig. 3. The water tends to push the dam to the right in Fig. 7, to increase the contact length with the foundation, and to

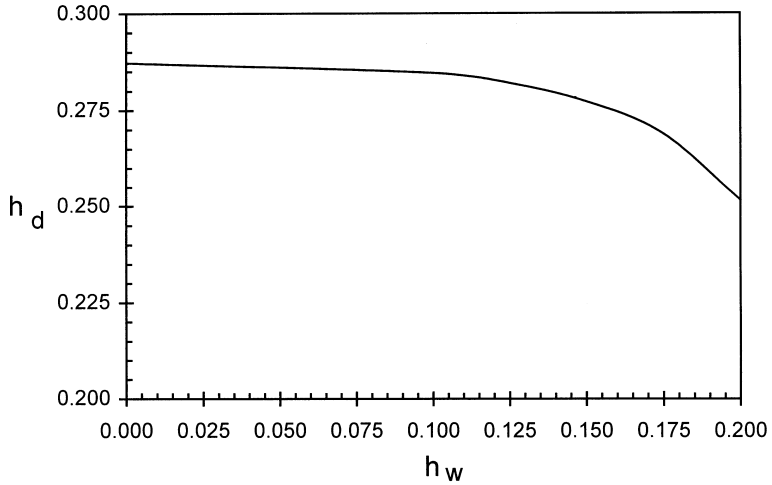

Fig. 8. Influence of external water height on height of folded dam for $\gamma = 30{,}000$ and $p = 3000$.

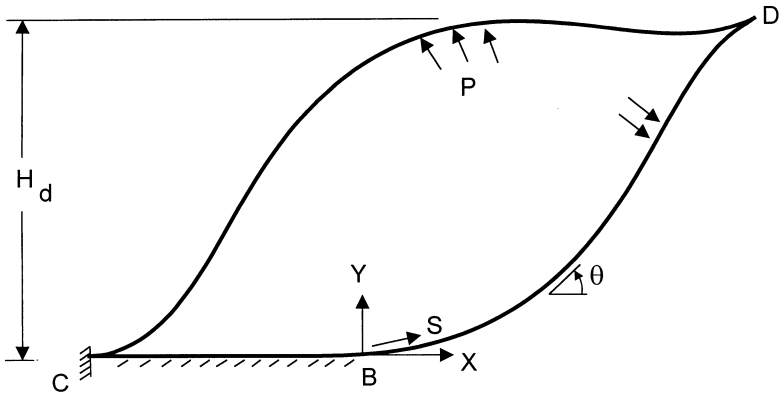

Fig. 9. Geometry of dam with fin.

decrease the height h_d of the dam. The variation of h_d with the water height h_w is presented in Fig. 8 for the same values of γ and p as used in Fig. 7.

3. Dam with fin

3.1. *Without external water*

The pressurized cross section of this type of dam is sketched in Fig. 9, in the absence of external water. The fin at D is at the midpoint of the perimeter from the clamped end C, and the origin is taken at the lift-off point B. Equations (4a–c) and (8a,b) govern on segment BD $(0 < s < s_D)$

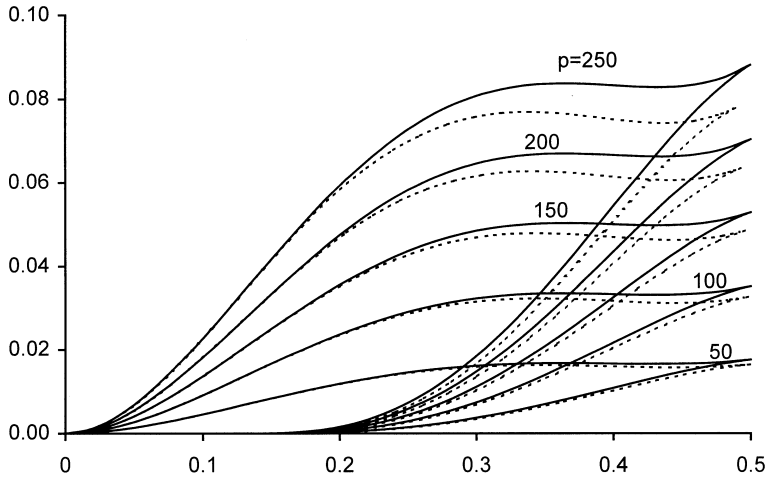

Fig. 10. Comparison of equilibrium shapes of dam with fin using linear analysis (solid) and elastica analysis (dashed).

except that p is replaced by $-p$ in (8b). For segment DC ($s_D < s < s_C$), θ, t, v, and m are defined so that they are continuous at D. This causes changes in the governing equations, which become

$$\frac{dx}{ds} = -\cos\theta, \quad \frac{dy}{ds} = -\sin\theta, \quad \frac{d\theta}{ds} = m, \quad \frac{dm}{ds} = -v, \quad \frac{dv}{ds} = p + (t_0 - m_D^2)m + \frac{1}{2}m^3, \qquad (9a\text{–}e)$$

where m_D is the value of the nondimensional bending moment m at the fin. At B, $x = y = \theta = m = 0$, and at C, $y = \theta = 0$ along with the length condition $x(s_C) = s_C - 1$. The unknowns are $z = (v(0), t_0, s_C)$ and the nonlinear system is

$$J(z) = (y(s_C; z), \theta(s_C; z), x(s_C; z) - s_C + 1) = 0.$$

The adjoint equations for (4a–c), (8a,b), (9a–e) do not exist because of the singularity at the fin. Nevertheless, finite difference approximations to the Jacobian matrix of $J(z)$ were adequate for the quasi-Newton code HYBRD from MINPACK (Moré et al., 1980) to work. This particular formulation was also well conditioned.

The dashed curves in Fig. 10 show the equilibrium shapes for small values of internal pressure p, while Fig. 11 depicts shapes at higher values of p. The solid curves in Fig. 10 correspond to solutions obtained from a linear analysis, assuming small slopes and Euler–Bernoulli beam theory. It leads to the following nondimensional displacements $y_1(x)$ and $y_2(z)$ for the lower and upper uplifted segments, respectively, where z is the horizontal axis with origin at C ($z = x + 0.131$):

$$y_1(x) = 0.0224px^3 - \tfrac{1}{24}px^4, \quad 0 < x < 0.369, \qquad (10a)$$

$$y_2(z) = 0.0131pz^2 - 0.0442pz^3 + \tfrac{1}{24}pz^4, \quad 0 < z < 0.5. \qquad (10b)$$

The linear solution is fairly accurate for the case $p = 50$, and also close to the nonlinear solution near the clamped end for the other cases in Fig. 10 (note that the horizontal and vertical scales are not the same in this figure).

The variation of the nondimensional height h_d of the dam with the internal pressure p is plotted

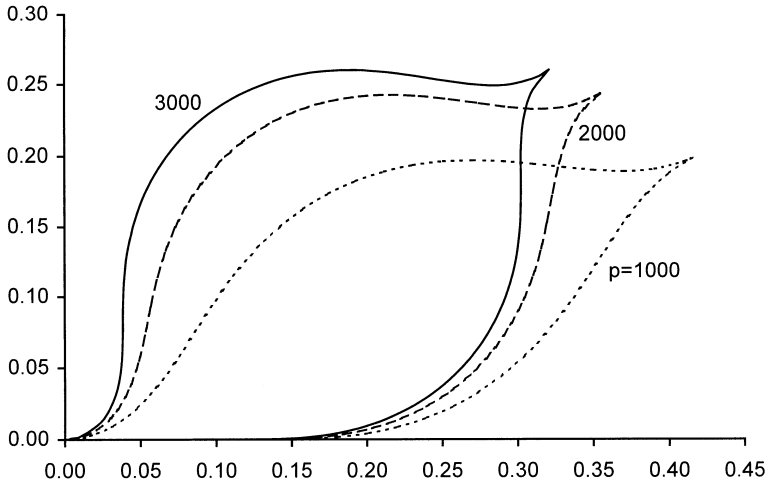

Fig. 11. Equilibrium shapes of dam with fin and no external water.

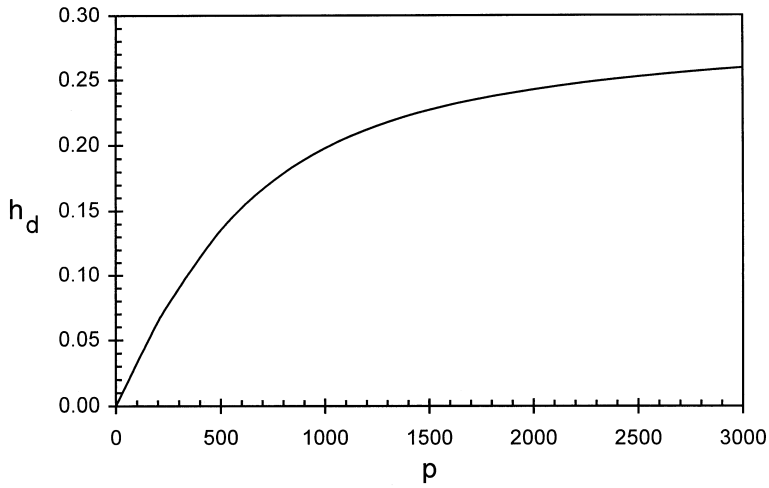

Fig. 12. Influence of internal pressure on height of dam with fin and no external water.

in Fig. 12. For the range shown, h_d corresponds to a point between C and D in Fig. 9, and not to the height of the fin. Here $h_d = 0$ when $p = 0$, unlike the case of the folded dam. The tension parameter t_0 is equal to 101, 248, and 396 for $p = 1000$, 2000, and 3000, respectively.

3.2. *With external water*

Next, external water is applied to the dam in Fig. 9, in the manner shown in Fig. 5. The coordinate system is chosen as in Fig. 5, with the fin at point D as in Fig. 9. The governing

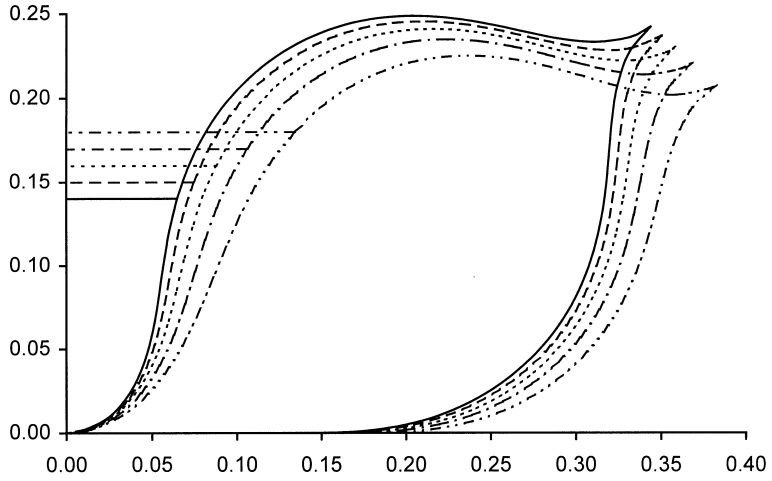

Fig. 13. Influence of external water on equilibrium shape of dam with fin for $\gamma = 30{,}000$ and $p = 3000$.

equations for segments CA and AD are the same as described in Section 2.2. For segment DB, the equations are (9a–e) except that p is replaced by $-p$ in (9e).

The unknowns here are $z = (\theta(0), m(0), v(0), t_0, s_B, s_C)$ and the nonlinear system to be solved is

$$J(z) = \begin{bmatrix} y(s_b; z) + h_w \\ \theta(s_B; z) \\ m(s_B; z) \\ y(s_C; z) + h_w \\ \theta(s_C; z) \\ x(s_B; z) - x(s_C; z) + s_B - s_C - 1 \end{bmatrix} = 0,$$

where $s_D = 0.5 + s_C$ (since $s_C < 0$). The same numerical algorithm as described in Section 3.1 is used here.

Some equilibrium shapes are shown in Fig. 13. As in Fig. 7, $\gamma = 30{,}000$ and $p = 3000$. The water heights in Fig. 13 are $h_w = 0.14, 0.15, 0.16, 0.17$, and 0.18. The tension parameter t_0 decreases from 381 to 348 as h_w increases from 0.14 to 0.18. Figure 14 demonstrates how the height of the dam decreases as the external water height increases.

4. Spillway gate without fin

In this section and the following one, an inflated bladder lifts a flat, rigid plate which holds back water. The geometry shown in Fig. 15 is considered first. The formulation is similar to that in Section 2. The elastica is attached at C to a rigid, horizontal foundation, and the other end is lifted, folded back, and again connected at C, but allowed to have a slope there. Internal pressure P is applied. A plate, pinned at C, rests on the bladder and impounds water. The plate has length L_p and weight per unit are a W_p.

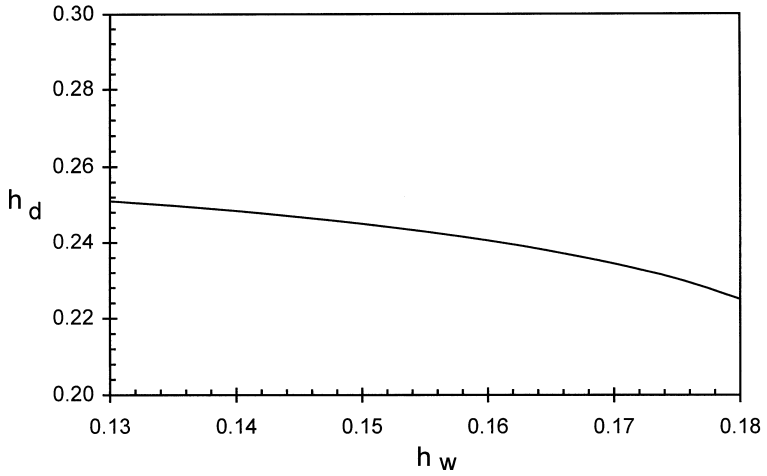

Fig. 14. Influence of external water height on height of dam with fin for $\gamma = 30{,}000$ and $p = 3000$.

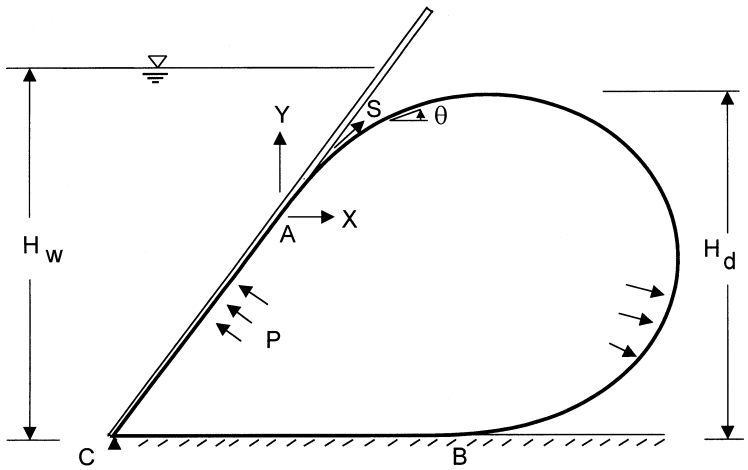

Fig. 15. Geometry of spillway gate without fin.

From A to B in Fig. 15, the governing equations are (4a–f) except that p is replaced by $-p$. For simplification in this case, (4a,b) are used in (4d,e) and the resulting equations are integrated to give

$$f = f_A + py, \quad g = g_A + px. \tag{11a,b}$$

Then the equations to be used are

$$\frac{dx}{ds} = \cos\theta, \quad \frac{dy}{ds} = \sin\theta, \quad \frac{d\theta}{ds} = m, \quad \frac{dm}{ds} = (f_A + py)\sin\theta + (g_A + px)\cos\theta. \tag{12a–d}$$

At A ($s = 0$), $x = y = m = 0$.

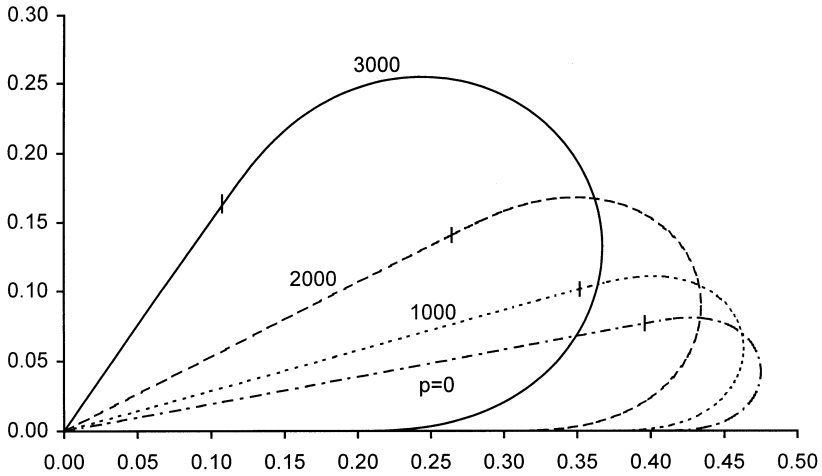

Fig. 16. Equilibrium shapes of spillway gate without fin for $r = 0$ and $u = 315$.

The unknowns are $z = (\theta(0), f_A, g_A, s_B)$, and the equations to be satisfied are

$$\theta(s_B; z) + \pi = 0, \quad m(s_B; z) = 0, \tag{13a,b}$$

$$(x(s_B; z) + s_B - 1)\sin(\theta(0)) - (1 + \cos(\theta(0)))y(s_B; z) = 0, \tag{13c}$$

$$r\sin(\theta(0)) + 3u\sin^2(\theta(0))\cos(\theta(0)) - 3p(y(s_B; z))^2 - 6(f_A\sin(\theta(0)) + g_A\cos(\theta(0)))y(s_B; z)\sin(\theta(0)) = 0, \tag{13d}$$

where

$$r = L\Gamma H_w^3/D, \quad u = LL_p^2 W_p/D. \tag{14a,b}$$

Equation (13c) comes from multiplying $\sin(\theta(0))$ times the condition that the perimeter is unity, whereas (13d) is a result of multiplying $6\sin^2(\theta(0))$ times moment equilibrium about C of a free body diagram of the plate. The equations (13a–d) were solved by a combination of homotopy and quasi-Newton methods, as described earlier in Section 2.

First, external water is not included ($r = 0$). For the case $u = 315$, results are presented in Figs 16 and 17. Equilibrium shapes are depicted in Fig. 16 for four values of internal pressure, including zero (when only the bending stiffness of the bladder holds up the plate). Vertical dashes indicate point A where the bladder loses contact with the plate. The nondimensional tension t_A per unit width at A (and also t_B at B) is 36.8, 84.1, 191, and 397 for $p = 0$, 1000, 2000, and 3000, respectively. The angle $\theta(0)$ of the plate with the horizontal is plotted as a function of p in Fig. 17, along with the length s_B of the elastica from A to B in Fig. 15 and its height h_d.

Next, with $u = 315$ and $p = 3000$, external water is applied to the plate. Figure 18 shows equilibrium shapes of the bladder for $r = 0$ (also the solid shape in Fig. 16), 25, 50, and 75. The corresponding values of t_A (and t_B) are 397, 367, 349, and 333. As expected, the plate is pushed downward and the contact lengths of the elastica with the plate and the foundation increase as the height of the water is increased.

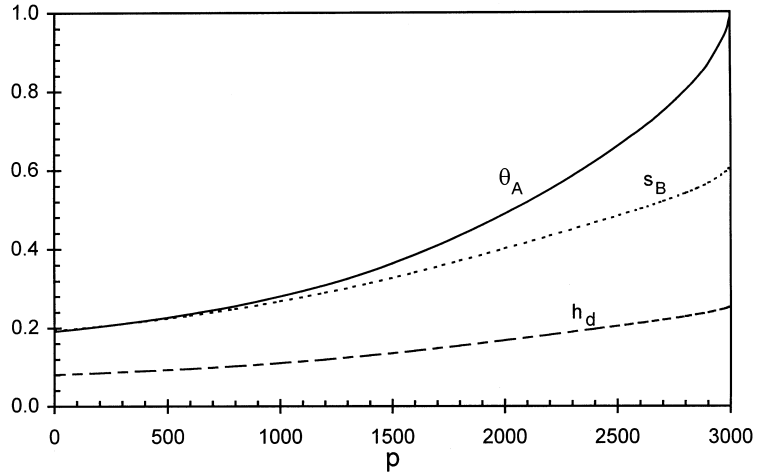

Fig. 17. Influence of internal pressure on plate angle, curved length of elastica, and height of elastica.

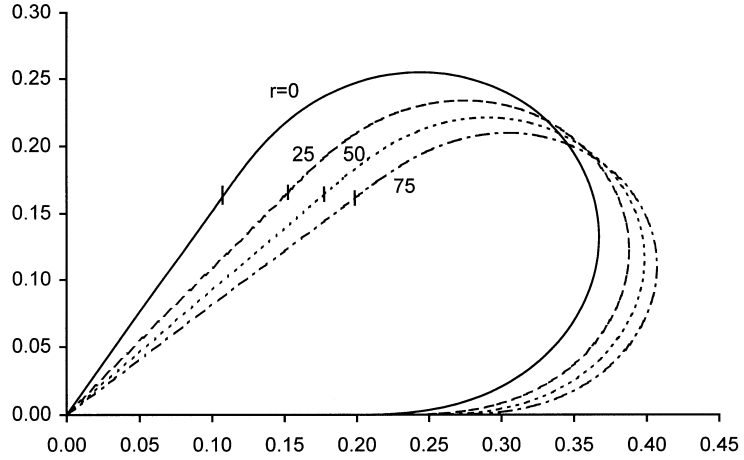

Fig. 18. Influence of external water on equilibrium shape of spillway gate without fin for $u = 315$ and $p = 3000$.

5. Spillway gate with fin

Finally, the bladder is modeled as in Section 3. The geometry is similar to that in Fig. 15 except that there is a fin at D, as in Fig. 9. The lengths of the upper and lower portions of the elastica from C to D are $L/2$ dimensionally, as before.

Two coordinate systems are used. In nondimensional terms, one of them involves s^*, x^*, y^*, and θ^*, with its origin at the lift-off point B as in Fig. 1. The other has its origin at point A in Fig. 15, where the elastica separates from the rigid plate, and involves s, x, y, and θ. Equations (12a–d) govern from A to the fin at D. From B to D, the governing equations involve quantities with an asterisk and are the same as (12a–d) except that p is replaced by $-p$, f_A by f_B^*, and g_A by g_B^*. At $s = 0$ (point A), $x = y = m = 0$, whereas at $s^* = 0$ (point B), $x^* = y^* = \theta^* = m^* = 0$.

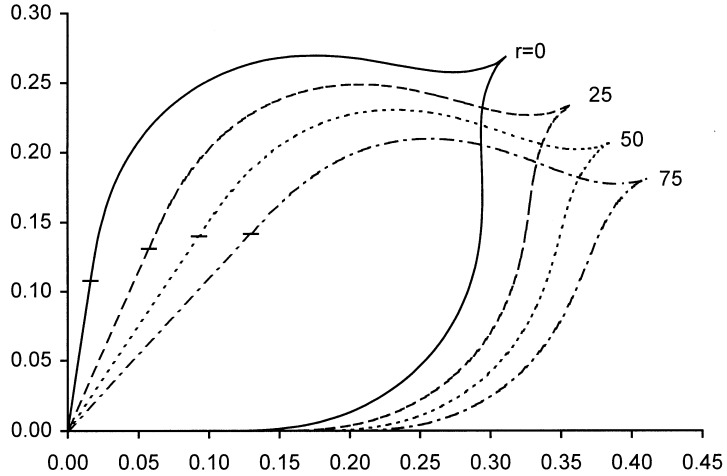

Fig. 19. Influence of external water on equilibrium shape of spillway gate with fin for $u = 20$ and $p = 3000$.

The unknowns are $z = (\theta(0), f_A, g_A, f_B^*, g_B^*, s_D, s_D^*)$. If the contact length from C to B on the foundation is denoted b and the contact length from C to A along the plate is denoted a, then

$$b = 0.5 - s_D^*, \quad a = 0.5 - s_D. \tag{15a,b}$$

The equations to be satisfied are (13d) with $y(s_B; z)$ replaced by $a \sin\theta(0)$, and

$$b + x(s_D^*; z) = a\cos(\theta(0)) + x(s_D; z), \quad y(s_D^*; z) = a\sin(\theta(0)) + y(s_D; z),$$
$$\theta(s_D^*; z) = \theta(s_D; z), \quad m(s_D^*; z) = -m(s_D; z), \quad f_B^* - py(s_D^*; z) + f_A + py(s_D; z) = 0,$$
$$g_B^* - px(s_D^*; z) + g_A + px(s_D; z) = 0, \tag{16a–f}$$

which involve continuity and equilibrium conditions. The numerical solution procedure is similar to that for the dam with fin in Section 3.2.

Figure 19 illustrates equilibrium shapes for $u = 20$, $p = 3000$, and the four values of r used in Fig. 18. Horizontal dashes on the curves indicate point A. The values of t_A (and t_B) are -87.6 (compression), 11.3, 64.0, and 98.9 for $r = 0$, 25, 50, and 75, respectively. The contact lengths increase as the height of the external water increases (for a given plate and a given internal pressure).

6. Concluding remarks

Most earlier studies of inflatable dams considered anchoring along two generators of the cylindrical structure, since this was the common mode of construction. At present, these dams are usually anchored along a single generator. The shapes of the cross sections of such dams have been examined in this study.

The cross section is modeled as an inextensible elastica. The analysis is challenging because the governing differential equations are highly nonlinear, and because the contact length along the

rigid foundation is unknown. For the spillway gate, the contact length of the rigid gate with the elastica is an additional unknown. Also, the problem is often very sensitive to the choices of the unknown parameters and unknown "initial conditions" at the origin of the coordinate system. Simple shooting and even quintic spline collocation did not always succeed, and more involved techniques such as globally convergent homotopy methods were required in some cases.

Inflatable dams have been constructed for a variety of purposes. However, they have not been used to protect towns, critical facilities, or homes from floodwaters. This study is part of an effort to investigate the feasibility of such an application for inflatable dams and for gates supported by pressurized bladders.

Acknowledgements

This research was supported by National Science Foundation Grants CMS-9422248 and DMS-9625968, and by Air Force Office of Scientific Research Grant F49620-96-1-0089.

References

Dakshina Moorthy, C.M., Reddy, J.N., Plaut, R.H., 1995. Three-dimensional vibrations of inflatable dams. Thin-Walled Structures 21, 291–306.

Hsieh, J.-C., Plaut, R.H., 1990. Free vibrations of inflatable dams. Acta Mechanica 85, 207–220.

Lloyd, D.W., 1984. The mechanics of drape. In Flexible Shells : Theory and Applications, ed. E. L. Axelrad and F. A. Emmerling, pp. 271–282. Springer-Verlag, Berlin.

Lloyd, D.W., Shanahan, W.J., Konopasek, M., 1978. The folding of heavy fabric sheets. Int. J. Mech. Sci. 20, 521–527.

Mahadevan, L., Keller, J.B., 1995. Periodic folding of thin sheets. SIAM Journal on Applied Mathematics 55, 1609–1624.

Moré, J.J., Garbow, B.S., Hillstrom, K.E., 1980. User Guide for MINPACK-1. ANL-80-74. Argonne National Laboratory, Argonne, IL.

Mysore, G.V., Liapis, S.I., Plaut, R.H., 1997. Vibration analysis of single-anchor inflatable dams. In Proceedings of the 4th International Symposium on Fluid-Structure Interactions, Aeroelasticity, Flow-Induced Vibration and Noise 2, 119–124. ASME, NY.

Plaut, R.H.. Liapis, S.L., Telionis, D.P., 1998. When the levee inflates. Civil Engineering 68, 62–64.

Sehgal, C.K., 1996. Design guidelines for spillway gates. Journal of Hydraulic Engineering 122, 155–165.

Stuart, I.M., 1966. A loop test for bending length and rigidity. Brit. J. Appl. Phys. 17, 1215–1220.

Tam, P.W.M., 1997. Use of rubber dams for flood mitigation in Hong Kong. Journal of Irrigation and Drainage Engineering 123, 73–78.

Wang, C.Y., 1981. Folding of elastica—similarity solutions. Journal of Applied Mechanics 48, 199–200.

Wang, C.Y., 1984. Post-buckling of horizontal heavy elastic sheet. Journal of Engineering Mechanics 110, 871–878.

Wang, C.Y., 1987. Elasto-plastic folding of thin sheets. Acta Mechanica 67, 139–150.

Watson, L.T., 1990. Globally convergent homotopy algorithms for nonlinear systems of equations. Nonlin. Dyn. 1, 143–191.

Watson, L.T., Sosonkina, M., Melville, R.C., Morgan, A. P., Walker, H.F., 1998. HOMPACK90 : A suite of Fortran 90 codes for globally convergent homotopy algorithms. ACM Trans. Math. Software, to appear.

Wu, P.-H., Plaut, R. H., 1996. Analysis of the vibrations of inflatable dams under overflow conditions. Thin-Walled Structures 26, 241–259.